hCG-induced endoplasmic reticulum stress triggers apoptosis and reduces steroidogenic enzyme expression through activating transcription factor 6 in Leydig cells of the testis

Sun-Ji Park[2,8,*], Tae-Shin Kim[1,8,*], Choon-Keun Park[3], Sang-Hee Lee[4], Jin-Man Kim[5], Kyu-Sun Lee[6], In-kyu Lee[7], Jeen-Woo Park[8], Mark A Lawson[1] and Dong-Seok Lee[2,8]

[1]Department of Reproductive Medicine, University of California, San Diego, 9500 Gilman Drives, La Jolla, California 92093, USA
[2]Center for Food and Nutritional Genomics Research, Kyungpook National University, Daegu, Republic of Korea
[3]Division of Animal Biotechnology, College of Animal Life Science, Kangwon National University, Chuncheon, Republic of Korea
[4]Department of Biological Sciences, Korea Advanced Institute of Science and Technology, Daejeon, Republic of Korea
[5]Cancer Research Institute and Department of Pathology, College of Medicine, Chungnam National University, Daejeon, Republic of Korea
[6]Aging Research Center, Korea Research Institute of Bioscience and Biotechnology, Daejeon, Republic of Korea
[7]Department of Internal Medicine, School of Medicine, Kyungpook National University, Daegu, Republic of Korea
[8]School of Life Sciences and Biotechnology, College of Natural Sciences, Kyungpook National University, Daegu 702-701, Republic of Korea
*(S-J Park and T-S Kim contributed equally to this work)

Correspondence should be addressed to D-S Lee
Email
lee1@knu.ac.kr

Abstract

Endoplasmic reticulum (ER) stress generally occurs in secretory cell types. It has been reported that Leydig cells, which produce testosterone in response to human chorionic gonadotropin (hCG), express key steroidogenic enzymes for the regulation of testosterone synthesis. In this study, we analyzed whether hCG induces ER stress via three unfolded protein response (UPR) pathways in mouse Leydig tumor (mLTC-1) cells and the testis. Treatment with hCG induced ER stress in mLTC-1 cells via the ATF6, IRE1a/XBP1, and eIF2α/GADD34/ATF4 UPR pathways, and transient expression of 50 kDa protein activating transcription factor 6 (p50ATF6) reduced the expression level of steroidogenic 3β-hydroxy-steroid dehydrogenase △5-△4-isomerase (3β-HSD) enzyme. In an *in vivo* model, high-level hCG treatment induced expression of p50ATF6 while that of steroidogenic enzymes, especially 3β-HSD, 17α-hydroxylase/C17–20 lyase (CYP17), and 17β-hydrozysteroid dehydrogenase (17β-HSD), was reduced. Expression levels of steroidogenic enzymes were restored by the ER stress inhibitor tauroursodeoxycholic acid (TUDCA). Furthermore, lentivirus-mediated transient expression of p50ATF6 reduced the expression level of 3β-HSD in the testis. Protein expression levels of phospho-JNK, CHOP, and cleaved caspases-12 and -3 as markers of ER stress-mediated apoptosis markedly increased in response to high-level hCG treatment in mLTC-1 cells and the testis. Based on transmission electron microscopy and H&E staining of the testis, it was shown that abnormal ER morphology and destruction of

Key Words
- ► Leydig cells
- ► Steroidogenic enzyme expression
- ► Activating transaction factor 6
- ► ER stress
- ► Testosterone

testicular histology induced by high-level hCG treatment were reversed by the addition of TUDCA. These findings suggest that hCG-induced ER stress plays important roles in steroidogenic enzyme expression via modulation of the ATF6 pathway as well as ER stress-mediated apoptosis in Leydig cells.

Introduction

Leydig cells, which are located between the seminiferous tubules of the testis, synthesize and secrete the hormone testosterone. Testosterone plays an important role in spermatogenesis (Haider 2004). It is well known that synthesis of testosterone is induced by LH, which is produced by the anterior pituitary gland, or human chorionic gonadotropin (hCG), which is secreted by the placenta. Both LH and hCG are heterodimeric glycoprotein hormones, and their molecular structures are almost identical. Further, LH and hCG bind to the same LH receptor and elicit identical biological responses. Accordingly, exogenous hCG has been used clinically to induce testosterone production in males (Ascoli *et al.* 2002, Keay *et al.* 2004).

Upon treatment with LH/hCG, intracellular levels of cAMP increase, promoting the transfer of cholesterol to the inner mitochondrial membrane through STAR protein. Following this, cholesterol is converted into pregnenolone via cytochrome P450 cholesterol side chain cleavage enzymes (P450scc/CYP11A1). Pregnenolone then moves out of the mitochondria and enters into the smooth endoplasmic reticulum (ER), where it is converted into progesterone by 3β-hydroxysteroid dehydrogenase △5-△4-isomerase (3β-HSD). Progesterone is subsequently metabolized to testosterone by 17α-hydroxylase/C17–20 lyase (CYP17) and 17β-hydrozysteroid dehydrogenase (17β-HSD). Importantly, to produce testosterone, steroidogenic enzymes such as those mentioned earlier are needed. It has been demonstrated that 3β-HSD and CYP17 are present exclusively in Leydig cells of mouse testis (Allen *et al.* 2004, Payne & Hales 2004). Moreover, adult Leydig cells display increased expression of steroidogenic enzymes, especially 3β-HSD and CYP17, as well as increased testosterone synthesis compared with immature Leydig cells (Chen *et al.* 2009). Thus, the ER of Leydig cells is involved in the synthesis of steroidogenic enzymes.

In eukaryotic cells, the ER plays an important role in the synthesis and folding of secretory and membrane proteins as it contains numerous chaperones and catalysts. Overload of ER functions, including excessive protein synthesis, Ca^{2+} homeostasis, and accumulation of unfolded and/or misfolded proteins in the ER lumen, results in ER stress through activation of the unfolded protein response (UPR). The UPR serves to alleviate ER stress, rescue ER homeostasis, and prevent cell death through the induction of ER chaperone expression, reduction of protein synthesis, and degradation of unfolded and/or misfolded proteins using three ER-localized transmembrane proteins: inositol-requiring protein-1 (IRE1 (ERN1)), protein kinase RNA (PKR)-like ER kinase (PERK), and activating transcription factor-6 (ATF6) (Schroder & Kaufman 2005).

Under ER stress conditions, the endoribonuclease IRE1 mediates unconventional splicing of X-box binding protein (*Xbp1*) mRNA into *sXbp1* mRNA, which is then translated into a functional transcriptional activator (Yoshida *et al.* 2001). IRE1 also induces pro-apoptotic Jun N-terminal kinase (JNK) signaling under ER stress conditions (Urano *et al.* 2000). In addition, PERK phosphorylates the α-subunit of eukaryotic translation initiation factor-2 (eIF2α; Shi *et al.* 1998). Phosphorylation of eIF2a leads to reduced protein translation as well as induction of ATF4 and pro-apoptotic CCAAT/enhancer-binding protein homologous protein (CHOP) expression (Jiang & Wek 2005). Furthermore, under ER stress, ATF6 translocates into the cis-Golgi compartment, where it is cleaved by site-1 and site-2 proteases (Ye *et al.* 2000). The active form of ATF6 (p50ATF6) then moves into the nucleus, where it acts as a transcription factor (Haze *et al.* 1999). Therefore, all three UPR pathways contribute to the induction of cell apoptosis, or ER stress-associated cell death, under conditions of excessive ER stress.

CHOP, JNK, and caspase-12 have been implicated in apoptotic signaling in response to ER stress. In mice, procaspase-12 is localized to the cytoplasmic side of the ER and is cleaved and activated specifically upon ER stress (Nakagawa & Yuan 2000, Nakagawa *et al.* 2000, Lai *et al.* 2007). Generally, professional secretory cells possess a well-developed ER structure, which is required for the vigorous synthesis of proteins. Thus, ER stress is mainly

Published by Bioscientifica Ltd.

studied in active secretory cells (Do *et al.* 2009, Malhi & Kaufman 2011, Kim *et al.* 2012). Leydig cells of the testis are another type of endocrine secretory cells characterized by heavy testosterone synthesis and secretion upon LH/hCG stimulation. Specifically, LH/hCG stimulation of Leydig cells increases steroidogenic enzyme expression, which is continuously necessary for the biosynthesis of testosterone in Leydig cells. Therefore, it can be hypothesized that the UPR may play a significant role in regulating steroidogenic enzyme expression upon hCG stimulation in Leydig cells.

In a clinical setting, hCG hormone is prescribed to increase natural testosterone production for the treatment of male sexual dysfunction and age-related testicular impairment (Namiki 1996, Depenbusch *et al.* 2002). Maintaining a durable pharmacological effect *in vivo* requires that a patient visit the hospital in short intervals in order to receive i.m. injections two or three times per week (Okabe *et al.* 2000). However, the side effects of such treatments have not been extensively evaluated. Interestingly, although Leydig cells produce and secrete testosterone in response to LH/hCG, repetitive hCG injection into mice has been shown to elicit a similar or lower testosterone level than that of control (Neaves 1978). Repeated hCG treatment raises H_2O_2 levels, induces apoptosis of Leydig and germ cells, and decreases testosterone release in rat testis (Gautam *et al.* 2007, Aggarwal *et al.* 2009, 2010, 2012). These observations showed that repeated and/or excessive hCG treatment seems to heavily damage steroidogenesis in Leydig cells. However, functional changes in the ER during steroidogenic enzyme expression in Leydig cells have not been demonstrated upon prolonged hCG treatment.

Therefore, in this study, we examined whether hCG induces ER stress through three UPR pathways (IRE1, PERK, and ATF6) as well as whether excess hCG treatment induces ER stress-mediated apoptosis in mouse Leydig tumor cells (mLTC-1) and mouse testis. We also investigated the role hCG-induced ER stress plays in steroidogenic enzyme expression as well as whether the ATF6 pathway of the UPR regulates hCG-stimulated steroidogenic enzyme expression in mLTC-1 cells and mouse testis.

Materials and methods

Chemicals

hCG was purchased from Intervet (Chorulon, Milton Keynes, Buckinghamshire, UK). 8-Bromo-cAMP (8-Br-cAMPs), brefeldin A (BFA), and thapsigargin (Tg) were purchased from Sigma.

Tunicamycin (Tm) and tauroursodeoxycholic acid (TUDCA) were purchased from Calbiochem (La Jolla, CA, USA).

Cell culture and *in vitro* transient transfection

The mLTC-1 mouse Leydig tumor cell line was purchased from the American Type Culture Collection (ATCC, Manassas, VA, USA). Cells were cultured in 5% CO_2 at 37 °C in RPMI 1640 (Wellgene, Daegu, Korea) supplemented with 1% penicillin/streptomycin (Invitrogen) and 10% fetal bovine serum (Hyclone, Thermo Scientific, Inc., Pittsburgh, PA, USA) (Rebois 1982, Manna *et al.* 2002). Transfections were carried out using Effectene (Qiagen, Inc.) transfection reagent according to the manufacturer's specifications. Cells were sub-cultured at a density of 2.5×10^5 cells/well in six-well plates and transfected with the appropriate indicated amounts of expression plasmids for ATF4, p50ATF6, and spliced XBP1 (a gift from PhD Inkye Lee) (Seo *et al.* 2008). At 48 h following transfection, cells were pre-treated with serum-free medium for 12 h and treated with 5 IU/ml hCG.

Transfection of siRNA for ATF6

Two predesigned potential *Atf6* siRNAs were chemically synthesized by Bioneers (Seoul, Korea), deprotected, and annealed. mLTC-1 cells were transfected with *Atf6* siRNA (100 nM) and control siRNA (100 nM) using Lipofectamine RNAiMAX according to the manufacturer's instructions. Treatment with hCG was performed at 48 h after siRNA transfection. Sequences of *Atf6* and non-specific control siRNAs were as follows: mouse *Atf6* siRNA, #1: CGA GAG UCU GCU UGC CAG U (sense), #2: CUG AAC UAU GGG CCC AUG A (sense); non-specific control siRNA, CCU ACG CCA CCA CUU UGG U (sense).

Cell viability by MTT assay and apoptosis analysis

Viability of mLTC-1 cells was determined by 3-(4,5-dimethylthiazol-2-yl)-2,5-diphenyltetrazolium bromide (MTT) assay (Mosmann 1983) using an Ultrospec 2100-pro spectrophotometer (Amersham Biosciences) at 570 nm. Percent viability was calculated according to the formula: (OD of hCG treated sample/OD of control)×100, as a reference. Apoptotic cells were identified based on characteristic bright blue fluorescence of nuclei that appears when condensed or fragmented chromatin is present (Newhouse *et al.* 2004). To visualize nuclear morphology, cells were fixed in methanol and stained with 1 μg/ml of the DNA dye Hoechst 33258 (Bisbenzimide, Sigma).

Western blot analysis

Lysates of mLTC-1 cells and total testis tissue were prepared in ice-cold PRO-PREP buffer (iNtRON Biotechnology, Inc., Daejeon, Korea). Proteins were separated on 12% SDS–polyacrylamide gels and then transferred to NitroBind nitrocellulose (Osmonics, Inc., Westborough, MA, USA). The membrane was blocked by blocking buffer and incubated with the following antibodies: anti-Grp78/BiP, anti-phospho-eIF2α, anti-SAPK/JNK, anti-phospho-SAPK/JNK, anti-caspase-3, anti-CHOP (Cell Signaling, Beverly, MA, USA), anti-p90ATF6 (Millipore, Bedford, MA, USA), anti-p50ATF6 (obtained from PhD InKyu Lee), anti-phopho-IRE1α (Abcam, Cambridge, MA, USA), anti-GADD34, anti-CREB2, anti-caspase-12, and anti-3β-HSD (Santa Cruz Biotechnology). Following incubation, membranes were washed and incubated with anti-goat, anti-rabbit, and anti-mouse IgG conjugated with HRP for 1 h at room temperature. After the removal of excess antibodies by washing, specific binding was detected using an ECL kit (Abfrontier, Seoul, Korea). Anti-β-actin antibody (Abfrontier) was used as a loading control. Band intensities were analyzed using Multi Gauge version 3.0 software (Fuji, Tokyo, Japan).

RNA extraction, RT-PCR, and splicing of Xbp1 mRNA analysis

Total RNA was isolated from both mLTC-1 cells and testis tissue using TRI solution (Bio Science Technology, Gyeongsan, Korea) according to the manufacturer's instructions. The cDNA was synthesized using 1 μg of each total RNA and AccuPower RT-PCR Premix (Bioneer, Seoul, Korea). PCR was carried out using AccuPower PCR Premix (Bioneer) containing specific primers for ER stress markers and steroidogenic enzymes (Supplementary Table 1, see section on supplementary data given at the end of this article). Conditions for the PCRs were as follows: 95 °C for 5 min, 95 °C for 30 s, 55–65 °C for 30 s, 72 °C for 30 s, and 72 °C for 5 min for 25–35 cycles. For analysis of *XBP1* splicing, PCR was carried out using 2× PCR Premix (Enzynomics, Seoul, Korea) containing specific primers (Supplementary Table 1). The PCR products were digested by Pst1 for 90 min at 37 °C. Each reaction mixture was electrophoresed on 2% agarose gel.

Testosterone assay by EIA

To measure testosterone levels, mLTC-1 cell culture media were collected after respective cell treatments in serum-free culture medium, and blood was collected from the orbital sinus of an ICR male mouse after respective administration. Medium and serum were separated by centrifugation at 12 000 g for 15 min at 4 °C and then stored at −70 °C until testosterone assays. Testosterone production was assessed using a testosterone enzyme immunoassay (EIA) kit (Enzo Life Sciences, Inc., Plymouth Meeting, PA, USA) according to the manufacturer's instructions. Testosterone concentration of each sample was calculated using the standard graph and expressed in ng/ml.

Administration of hCG, Tm, and TUDCA in male mice

Male ICR mice (10 weeks of age) were purchased from Hyochang Bio-Science (Daegu, Korea) and maintained in accordance with the institutional guidelines of the Institutional Animal Care and Use Committee of the Korea Research Institute of Bioscience and Biotechnology (KRIBB, Daejeon, South Korea). ICR mice were administered hCG (0.05 and 0.5 IU/g BW) and Tm (0.2 and 1.0 μg/g BW) by i.p. injection once per day for the indicated periods. TUDCA as an ER stress inhibitor was administered two times per day in two doses (250 mg/kg at 0800 and 2000 h, total of 500 mg/kg per day). Control was administered by i.p. injection with saline.

Construction of lentiviral vector (LV) and LV-mediated gene transfer into testis *in vivo*

Full-length *p50Atf6* cDNA fragment from p50ATF6 vector was amplified by PCR. The purified fragment was inserted into pLenti 6.3/V5-DEST (Invitrogen) by following the manufacturer's instructions. Finally, pLV-p50ATF 6 vector was constructed. pLV-Turbo-GFP as a positive control was purchased from Sigma. Lentiviruses were packaged in HEK293T cells and titrated by ELISA for viral capsid protein (p24), as described previously (Kim *et al*. 2010). Thus, highly concentrated lentiviruses were injected into ICR mouse testis by following a previously reported method (Kim *et al*. 2010). Testes were injected with 20 μl of LV (7 ng of p24s/μl) by gentle syringe pressure using sharpened glass microcapillary pipettes.

Hematoxylin and eosin staining and transmission electron microscopy

Testes of male ICR mice after respective administration were analyzed by hematoxylin and eosin (H&E) staining as well as transmission electron microscopy (TEM). First,

testes isolated from mice were fixed with 4% formalin (Sigma) overnight, embedded in paraffin, and processed into sections of 5 μm thickness. The sections were then subjected to H&E staining in order to examine morphological features using standard methods. For TEM, the testes were fixed with 4% glutaraldehyde in 0.1 M phosphate buffer (pH 7.4). Fixed testes were then postfixed in 1% osmium tetroxide in 0.1 M cacodylate buffer for 1 h at 4 °C. Following this, testes were washed briefly in 0.1 M cacodylate buffer, dehydrated through a graded ethanol series, infiltrated using propylene oxide and EPON epoxy resin (Structure Probe, West Chester, PA, USA), and finally embedded in Beam capsules. Polymerization of the testes was then carried out at 60 °C for 48 h. Thin sections were cut with a diamond knife on an ULTRACUT UCT ultramicrotome (Leica, Vienna, Austria) and mounted on formvar-coated slot grids. Unstained sections were observed under a Tecnai G2 Spirit Twin transmission electron microscope (FEI Company, Hillsboro, OR, USA).

Statistical analysis

Data are presented as mean $\pm$ s.e.m. of three or more independent experiments. For group comparisons, one-way ANOVA followed by Dunnett's multiple comparison tests were performed using the Prism software package version 4.0 for statistical data analysis (GraphPad Software, Inc., La Jolla, CA, USA). Differences are considered significant at $P < 0.05$.

Results

hCG induces apoptotic cell death in mLTC-1 cells

To demonstrate whether hCG stimulation leads to death of mLTC-1 cells, we first treated mLTC-1 cells with different doses (0, 0.5, 5, and 25 IU/ml) of hCG for various times (6, 12, and 24 h). We further analyzed cell viability by MTT assay. No significant change in cell viability was observed at 0.5 IU/ml hCG, whereas there was a significant decrease in cell viability at 5 IU/ml hCG and higher (Fig. 1A). The viability of mLTC-1 cells significantly decreased in a dose- and time-dependent manner. Specifically, cell viabilities were ~79.3 and 66.2% after treatment with 5 IU/ml hCG for 12 and 24 h respectively (Fig. 1B).

Furthermore, nuclear condensation of cells was observed under a fluorescence microscope by Heochest 33258 staining following 5 IU/ml hCG treatment for 12 and 24 h (Fig. 1C). According to this result, mLTC-1

cells displayed apoptotic features such as condensed nuclei after treatment with 5 IU/ml hCG for 24 h. The number of apoptotic mLTC-1 cells significantly increased upon 24 h hCG exposure compared with that of control (Fig. 1D). These results indicate that prolonged exposure to a high dose of hCG induced death of mLTC-1 cells via apoptosis.

hCG induces ER stress-mediated apoptosis in mLTC-1 cells

Disruption of ER homeostasis by stress induces expression of CHOP, phospho-JNK, and cleaved caspase-12, which mediates apoptotic signals. In turn, activated caspase-12 localized on the cytoplasmic side of the ER cleaves procaspase-9 into active caspase-9, which further cleaves and activates caspase-3, resulting in apoptosis (Morishima et al. 2002).

Therefore, to confirm whether hCG induces ER stress-mediated apoptosis in mLTC-1 cells, we treated with 5 and 25 IU/ml hCG as well as 2 μg/ml Tm (ER stress inducer) for 12, 18, and 24 h respectively. Then, GRP78/BIP (HSPA5) protein as a major ER stress sensor (Schroder & Kaufman 2005) along with CHOP, phospho-JNK, cleaved caspase-12, and cleaved caspase-3 as ER stress-mediated apoptosis markers were analyzed by western blot analysis. As shown in Fig. 2A and B, hCG and Tm treatment significantly induced expression of GRP78/BIP protein compared with that of control (0 IU/ml hCG). Levels of CHOP and cleaved caspase-12 significantly increased in a time-dependent manner upon 5 IU/ml hCG treatment (left panel, Fig. 2B), whereas 25 IU/ml hCG resulted in increases in CHOP and cleaved caspase-12 levels until 18 h, followed by decreases (right panel, Fig. 2B). Interestingly, whereas phospho-JNK levels increased markedly at 12 h, that of cleaved caspase-3 as an apoptosis marker significantly increased at 18 and 24 h after hCG treatment (Fig. 2A). This result was consistent with hCG-induced cell death via apoptosis (Fig. 1). These results indicate that hCG-induced cell death was the result of ER stress-mediated apoptosis.

hCG treatment in mLTC-1 cells leads to activation of unfolding protein response signaling

The UPR is a cellular stress response related to the ER. When the UPR is perturbed or insufficient to deal with current stress conditions, apoptotic cell death is initiated (Lai et al. 2007). Therefore, to investigate whether hCG-induced ER stress is mediated through UPR signaling in mLTC-1 cells, we examined the expression levels of phospho-eIF2α/GADD34/ATF4, phospho-IRE1/phospho-JNK/sXBP1, and p90ATF6/p50ATF6 by western blot
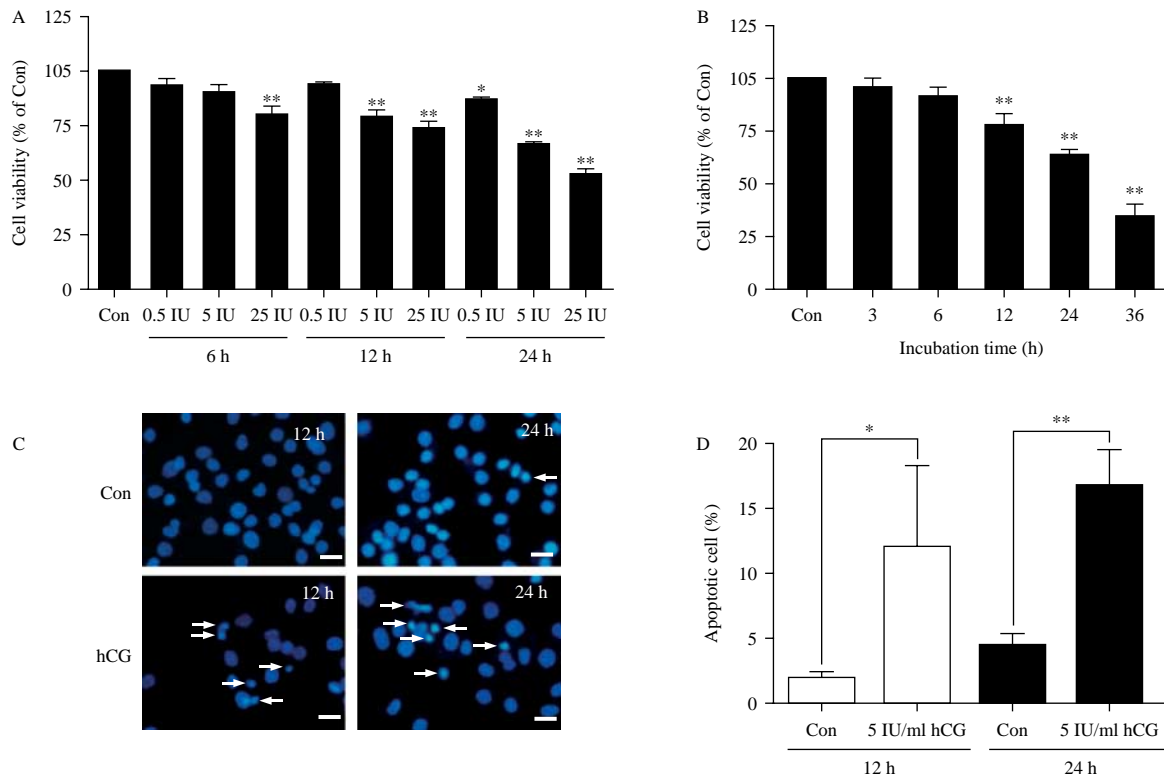
Figure 1

hCG induces cell death via apoptosis in mLTC-1 cells. (A) Cell viability analysis of mLTC-1 cells treated with 0.5, 5, and 25 IU/ml hCG for the indicated times. mLTC-1 cells were incubated in a dose- and time-dependent manner with hCG, and cell viability was analyzed by MTT assay. (B) mLTC-1 cells were incubated with 5 IU/ml hCG for the indicated times (0, 3, 6, 12, 24, and 36 h). Cell viability analysis of cells treated with 5 IU/ml hCG for different incubation times. (C) Nuclear condensation of mLTC-1 cells in the presence of 5 IU/ml hCG for 12 and 24 h, followed by visualization under a fluorescence microscope after Heochst 33258 staining for 10 min. White arrows indicate condensed nuclei as a marker of apoptotic cells. Scale bar: 30 μm. (D) Rate of apoptotic mLTC-1 cell death with/without 5 IU/ml hCG treatment for 12 and 24 h was determined by Heochst 33258 staining and analyzed by counting condensed nuclei in mLTC-1 cells. Data in the bar graph represent mean $\pm$ s.e.m. of four independent measurements. $*P < 0.05$; $**P < 0.01$, compared with control.

analysis in order to confirm the activation of three UPR pathways (PERK, IRE1, and ATF6). First of all, expression of the major ER stress marker GRP78/BIP protein dramatically increased at 3 h upon 5 IU/ml hCG treatment, followed by a gradual decrease in a time-dependent manner (upper panel, Fig. 3A).

For one UPR pathway, it has been reported that eIF2α is phosphorylated by PERK in response to ER stress, leading to attenuation of translation initiation and protein synthesis (Shi *et al.* 1998). Surprisingly, the level of phospho-eIF2α protein rapidly decreased after hCG treatment and then gradually increased (Fig. 3A). This result demonstrates that eIF2α was possibly phosphorylated in unstimulated mLTC-1 cells while its phosphorylation was reduced upon hCG-stimulated optimal expression of steroidogenic enzymes in Leydig cells. Upon phosphorylation of eIF2α in response to ER stress,

it has been reported that growth arrest and DNA damage-inducible protein (GADD34 (PPP1R15A)) positively dephosphorylates eIF2α, thereby inducing recovery from shutoff of protein synthesis (Kojima *et al.* 2003). Expression of GADD34 increased by 9 h following hCG treatment and decreased thereafter (Fig. 3A). This result suggests that GADD34 expression maintained homeostasis of hCG-induced steroidogenic enzyme expression in mLTC-1 cells. Further, ATF4 expression consistently increased after hCG treatment (Fig. 3A).

In addition, the expression of phospho-IRE1 protein, another ER stress indicator, dramatically increased by 3 h following hCG treatment, similar to that of GRP78/BIP, whereas the level of phospho-JNK increased until 9 h and decreased thereafter (Fig. 3A). During ER stress, mRNA encoding transcription factor *Xbp1* is spliced by the endoribonuclease IRE1. Subsequently, the spliced
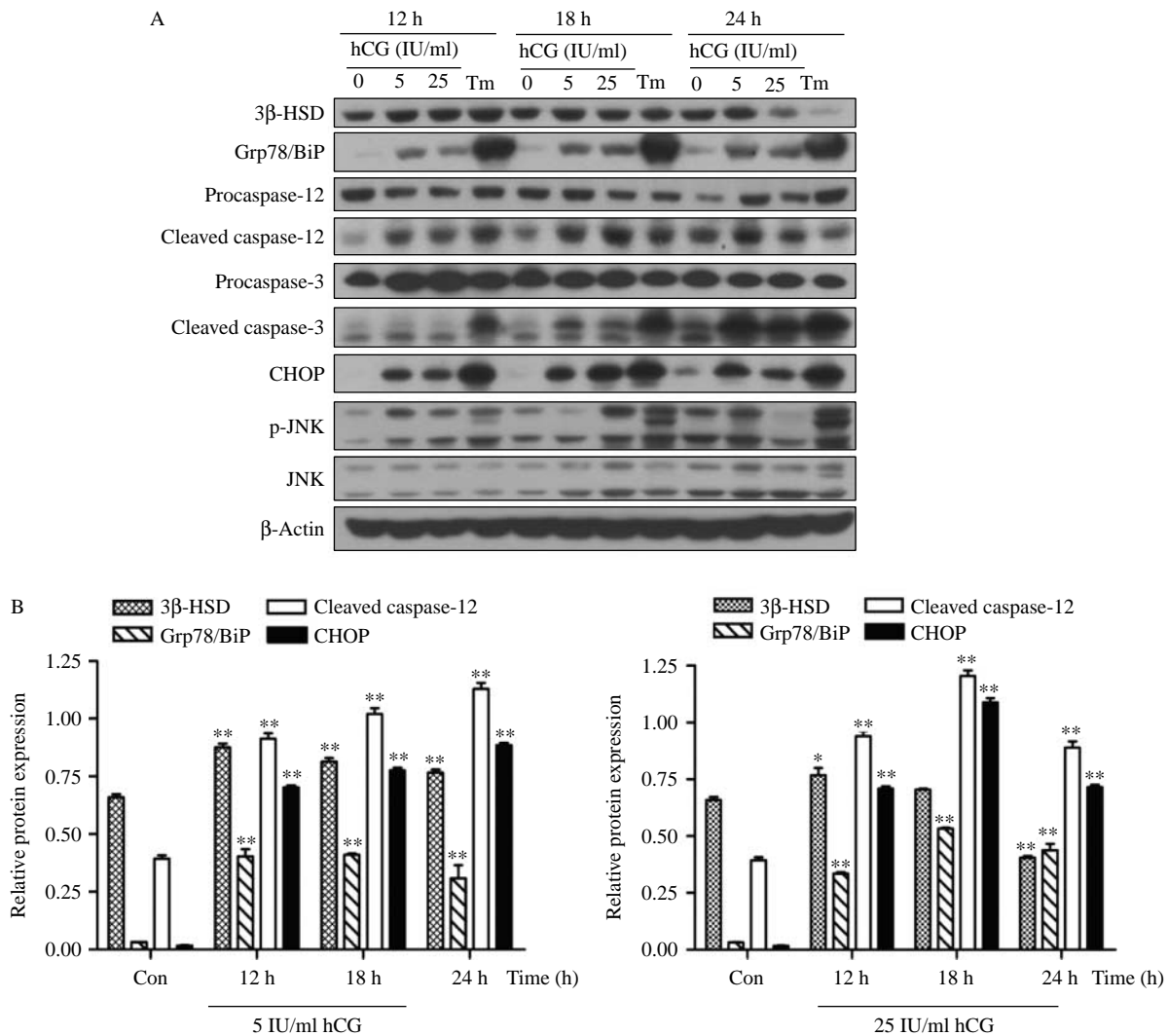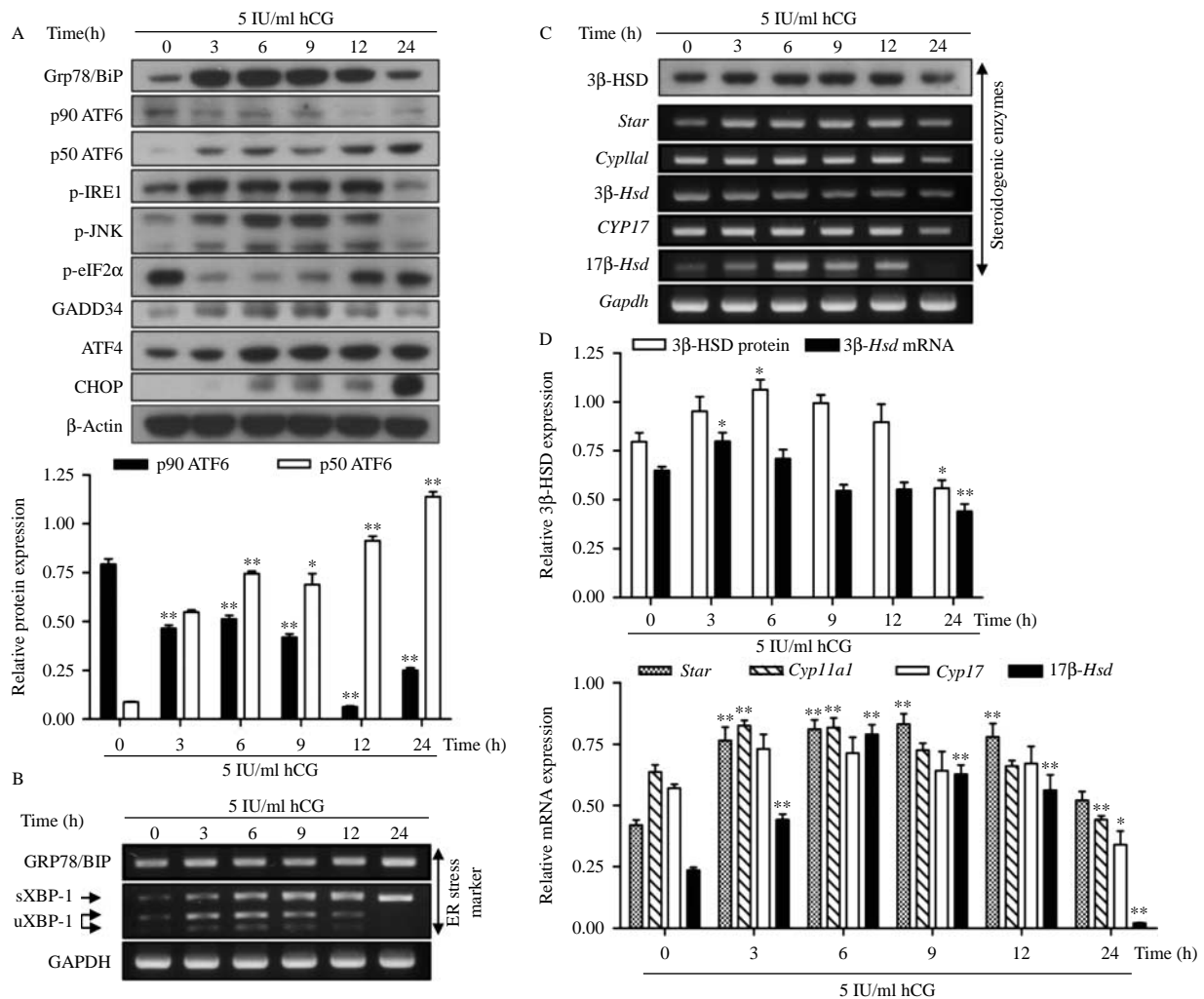
Figure 2

hCG induces ER stress-mediated apoptosis in mLTC-1 cells. (A) Western blot analysis of 3β-HSD, Grp78/BiP, procaspase-12, cleaved caspase-12, pro-caspase-3, cleaved caspase-3, CHOP, phospho-JNK, JNK, and β-actin proteins in mLTC-1 cells treated with hCG (0, 5, and 25 IU/ml) and Tm (2 μg/ml) for 12, 18, and 24 h after pre-incubation with serum-free medium for 12 h. (B) 3β-HSD, GRP78/BIP, cleaved caspase-12, and CHOP proteins were quantified and normalized to β-actin for western blot analysis. Graphs present the indicated periods for treatment with 5 IU/ml hCG (left panel) and 25 IU/ml hCG (right panel). Data in the bar graph represent mean ± s.e.m. of three independent measurements. *$P < 0.05$; **$P < 0.01$, compared with control.

Xbp1 (*sXbp1*) mRNA is translated into a functional transcriptional activator (Yoshida *et al.* 2001). To investigate whether hCG-induced phospho-IRE1 expression promotes alternative sXBP1 splicing in mLTC-1 cells, we used RT-PCR to detect alternative *sXbp1* mRNA transcript. We detected a time-dependent increase in the level of alternative *sXbp1* mRNA transcript in response to hCG-increased phospho-IRE1 levels (Fig. 3B).

As a third ER stress indicator, we investigated the expression levels of both p90ATF6 and p50ATF6. Protein expression levels of 90 kDa ATF6 (p90ATF6) and active 50 kDa ATF6 (p50ATF6) significantly decreased and increased respectively in mLTC-1 cells in a time-dependent manner in response to hCG treatment (upper and lower panels, Fig. 3A). As shown in Fig. 3A, expression of CHOP gradually increased early in a time-dependent manner following hCG treatment, whereas it significantly increased by 24 h. Further, expression of CHOP was induced by both ATF4 and p50ATF6. These results show that hCG treatment induced ER stress via the ATF6, IRE1a/XBP1, and elf2a/GADD34/ATF4 pathways in mLTC-1 cells. We also detected that cAMP as an

Figure 3

hCG treatment leads to activation of the unfolding protein response signaling in mLTC-1 cells. (A) Western blot analysis of GRP78/BIP, p90ATF6, p50ATF6, phospho-IRE1, phospho-JNK, phospho-eIF2a, GADD34, ATF4, CHOP, and β-actin proteins in mLTC-1 cells treated with hCG in a time-dependent manner. mLTC-1 cells were incubated with 5 IU/ml hCG for the indicated times (upper panel). Graph shows that p90ATF6 and p50ATF6 proteins were quantified and normalized to β-actin for western blot analysis (bottom panel). Data in the bar graph represent mean±s.e.m. of three independent measurements. *$P<0.05$; **$P<0.01$, compared with 0 h. (B) RT-PCR analysis of GRP78/BIP, spliced XBP1 (sXBP1), and unspliced XBP1 (uXBP1) as ER stress markers, and *Gapdh* mRNA as a control in mLTC-1 cells treated with 5 IU/ml hCG for the indicated times. (C) Western blot analysis of 3β-HSD protein and RT-PCR analysis of *Star*, *Cyp11a1*, *3β-hsd*, *Cyp17*, and *17β-hsd* mRNA as steroidogenic enzymes in mLTC-1 cells treated with 5 IU/ml hCG for the indicated times. (D) Graph shows that the 3β-HSD protein level was quantified and normalized to β-actin for western blot analysis. The *3β-hsd* mRNA level was quantified and normalized to GAPDH for RT-PCR analysis in mLTC-1 cells treated with 5 IU/ml hCG for the indicated times (upper panel). Graph shows that *Star*, *Cyp11a1*, *Cyp17*, and *17β-hsd* mRNA levels were quantified and normalized to GAPDH for RT-PCR analysis (bottom panel). Data in the bar graph represent mean±s.e.m. of three independent measurements. *$P<0.05$; **$P<0.01$, compared with 0 h.

intracellular second messenger of hCG stimulation led to the activation of UPR signaling via Grp78/BiP, ATF6, and XBP1 in mLTC-1 cells (Supplementary Figure 1, see section on supplementary data given at the end of this article).

We next investigated whether steroidogenic enzyme expression is affected by time of the hCG treatment. The protein level of 3β-HSD as well as mRNA levels of *3β-HSD* (*HSD3B6*), *CYP17* (*CYP17A1*), and *17β-HSD* (*HSD17B1*)

increased initially in response to hCG treatment, after which they gradually decreased (Fig. 3C and D). After 24 h of hCG treatment, mRNA levels of steroidogenic enzymes (*Star*, *Cyp11a1*, *3β-Hsd*, *Cyp17*, and *17β-Hsd*) markedly decreased in mLTC-1 cells (Fig. 3C and D). Furthermore, mRNA levels of steroidogenic enzymes markedly decreased in a time-dependent manner in cells treated with Tm, Tg, or BFA, which are ER stress inducers

(Nakagawa *et al.* 2000; Supplementary Figure 2, see section on supplementary data given at the end of this article). These results indicate that hCG treatment led to activation of UPR signaling for the maintenance of ER homeostasis upon hCG-stimulated optimal expression of steroidogenic enzymes, which is necessary for the biosynthesis of testosterone. However, prolonged hCG stimulation resulted in severe ER stress as well as reduced steroidogenic enzyme expression. Therefore, it was demonstrated that prolonged hCG stimulation reduced protein and mRNA expression levels of steroidogenic enzymes in mLTC-1 cells.

p50ATF6 mainly inhibits hCG-stimulated steroidogenic enzyme 3β-HSD expression in mLTC-1 cells

Although we confirmed the involvement of the three signaling pathways of the UPR (IRE1, PERK, and ATF6) in steroidogenic enzyme expression following hCG

treatment, it is still unclear which of the three different UPR signaling pathways is most responsible. Therefore, as p50ATF6, ATF4, and sXBP1 were shown to be key transcription factors in the ER stress response, we determined which of these most downregulates 3β-HSD expression as a major steroidogenic enzyme during testosterone production in response to hCG treatment.

For this, mLTC-1 cells were transfected with sXBP1, ATF4, and p50ATF6 expression vectors, after which the levels of sXBP1, ATF4, and p50ATF6 were confirmed in mLTC-1 cells by western blot or RT-PCR analysis (Supplementary Figure 3, see section on supplementary data given at the end of this article). The protein level of 3β-HSD profoundly decreased in cells transfected with p50ATF6 upon hCG treatment compared with those transfected with mock or other vectors (upper and lower panels, Fig. 4A).

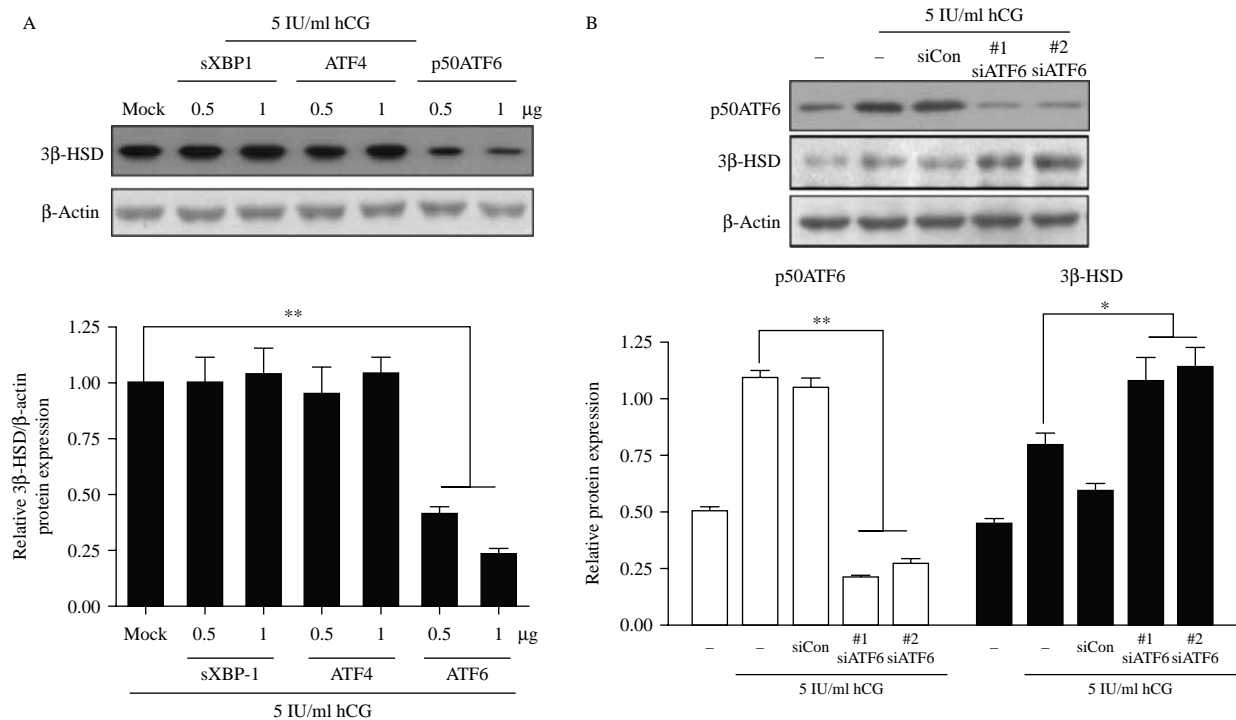To further confirm that the ATF6 pathway mediates suppression of 3β-HSD gene expression, we downregulated

Figure 4

p50ATF6 inhibits hCG-stimulated steroidogenic enzyme expression. (A) Western blot analysis of 3β-HSD protein as a marker of steroidogenic enzymes in mLTC-1 cells transfected separately with 0.5 and 1 μg sXBP1, ATF4, and p50ATF6 vectors (upper panel). Graph shows that 3β-HSD proteins were quantified and normalized to β-actin for western blot analysis (bottom panel). Data in the bar graph represent mean±s.e.m. of three independent measurements. **P<0.01, compared with control (mock). (B) mLTC-1 cells were transfected with two different siATF6

(#1 and #2) and siCon (as siRNA control), followed by treatment with 5 IU/ml hCG for 2 h. p50ATF6, 3β-HSD, and β-actin protein as a control were analyzed by western blot analysis (upper panel). Graph shows that p50ATF6 and 3β-HSD proteins were quantified and normalized to β-actin for western blot analysis (bottom panel). Data in the bar graph represent mean±s.e.m. of three independent measurements. *P<0.05; **P<0.01, compared with only 5 IU/ml hCG treatment.

endogenous *Atf6* expression by transfecting mLTC-1 cells with two types of siRNA-*Atf6*, followed by incubation in hCG-containing media. Transfection of the two siRNA-*Atf6* (#1 and #2) markedly reduced the hCG-induced increase in p50ATF expression. Further, the protein level of 3β-HSD was significantly higher in cells treated with siRNA-*Atf6* and hCG compared with those treated with control siRNA and hCG (upper and lower panels, Fig. 4B). These results demonstrate that hCG-induced ER stress via the ATF6 pathway alleviated expression of the steroidogenic enzyme 3β-HSD *in vitro*.

High-level hCG treatment induces ER stress-mediated apoptosis and damage to testicular histology, ER structure, and mitochondria in Leydig cells of mouse testis *in vivo*

To determine whether hCG induces ER stress-mediated apoptosis in the testis *in vivo*, we administered hCG (0.05 and 0.5 IU/g BW) or Tm (0.2 and 1.0 g/g BW) as an ER stress inducer to mice once per day for 3 days. First of all, we confirmed that 3β-HSD protein expression was upregulated upon low-level administration of hCG (0.05 IU/g BW) and downregulated in testes administered a high level of hCG (0.5 IU/g BW) and Tm (1.0 g/g BW) (Fig. 5A). Moreover, high-level administration of hCG to mice significantly induced the expression of cleaved caspases-12 and -3, CHOP, and phospho-JNK compared with control mice, but levels were restored by addition of TUDCA, an ER stress inhibitor (Fig. 5A). TUDCA is an endogenous bile acid that can be safely used as a hepatoprotective agent in humans having cholestatic liver diseases, and it alleviates ER stress in cells and whole animals by blocking calcium-mediated apoptotic pathways. TUDCA is also a chemical chaperone that can modulate ER function by protecting against UPR induction and ER stress-induced apoptosis (Xie *et al.* 2002, Ozcan *et al.* 2006). These results strongly demonstrate that high-level hCG administration caused ER stress-induced apoptosis in Leydig cells of mouse testis.

Moreover, it has been reported that Tm-mediated ER stress induces histological damage to tissues as well as the ultrastructure of cell organs (Xie *et al.* 2002). In this study, we analyzed the histology of the testis along with the ultrastructure of the ER and mitochondria in Leydig cells following administration of hCG and Tm with/without TUDCA. Histological analysis by H&E staining showed that testicular histology following low-level administration of hCG (0.05 IU/g BW) was not significantly affected compared with that of control (Fig. 5B vs
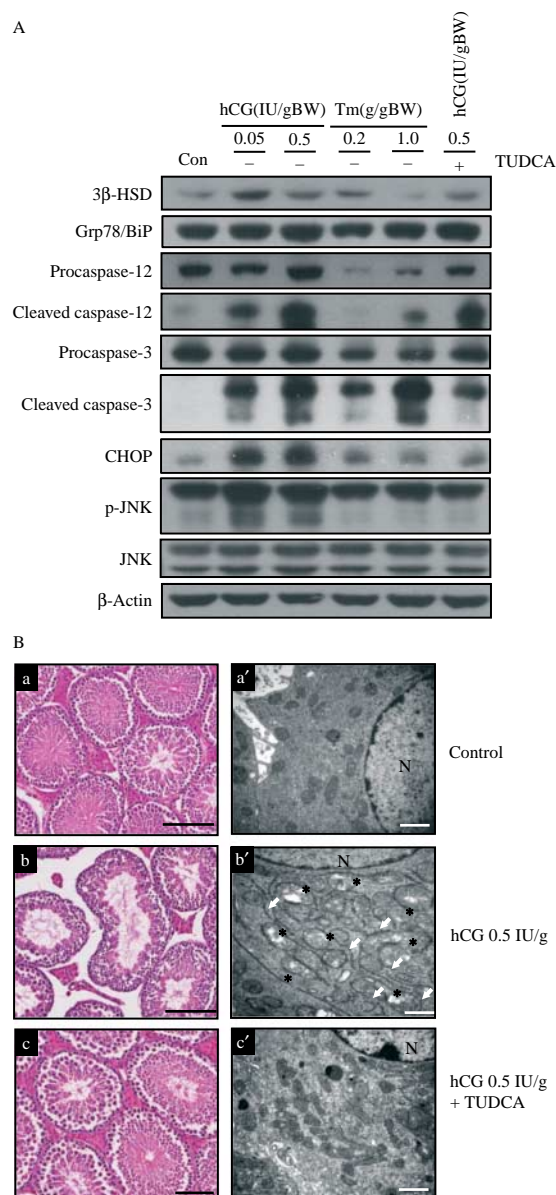

Figure 5
hCG induces ER stress-mediated apoptosis and abnormal morphology of ER, mitochondria *in vivo*. (A) Western blot analysis of 3β-HSD, ER stress-associated proteins (GRP78/BIP, procaspase-12, cleaved caspase-12, procaspase-3, cleaved caspase-3, CHOP, phosphor-JNK, JNK), and β-actin proteins in the testes of ICR mice administered hCG (0.05 and 0.5 IU/g BW) and Tm (0.2 and 1.0 μg/g BW) once per day for 3 days. TUDCA was applied intraperitoneally to mice treated with hCG (0.5 IU/g BW) at the same time points (250 mg/kg at 0900 and 2000 h, total 500 mg/kg per day). Controls were administered saline by i.p. injection. (B) (a, b and c) H&E staining of the testis section of mice treated with saline (a), hCG 0.5 IU/g BW; (b), and followed by addition of TUDCA (total 500 mg/kg/day; (c). a′, b′ and c′, TEM images of Leydig cells in testis treated with saline, hCG, and TUDCA. White arrow indicates fragmentation of ER lumen. Asterisks indicate severe loss of cristae and rarefaction of the mitochondrial matrix. N, nuclear. scale bar, 200 μm (a,b and c); 1 μm (a′,b′ and c′).

Supplementary Figure 4A, see section on supplementary data given at the end of this article), whereas high-level administration of hCG (0. 5 IU/g BW) damaged the interstitial space of seminiferous tubules as well as the inside of seminiferous tubules (Fig. 5B). The interstitial damage induced by high-level hCG treatment was similar to that observed upon Tm treatment (Supplementary Figure 4B). Further, disorders of the interstitial space induced by hCG and Tm treatment were protected against by TUDCA (Fig. 5B and Supplementary Figure 4C, respectively). On the other hand, TEM examination of the ER and mitochondrial ultrastructure in Leydig cells showed that low-level administration of hCG (0.05 IU/g BW) caused stacking of the ER (black arrow) around the nucleus compared with control cells (Fig. 5B vs Supplementary Figure 4a). However, disarranged fragments of the ER (white arrow), severe loss of cristae, and rarefaction of the mitochondrial matrix (asterisks) were observed in Leydig cells administered a high level of hCG (0. 5 IU/g BW) (Fig. 5B). Additionally, damage to the ER and mitochondria in Leydig cells induced by a high level of hCG was also attained by Tm treatment (Supplementary Figure 4b). Abnormal morphologies of the ER and mitochondria induced by high-level hCG and Tm treatment were slightly recovered by the addition of TUDCA (Fig. 5B and Supplementary Figure 4c). These results indicate that high-level hCG treatment induced damage to the testicular histology, ER morphology, and mitochondria of Leydig cells of mouse testis.

Administration of hCG upregulates p50ATF6 expression and downregulates steroidogenic enzymes in Leydig cells of the testis *in vivo*

To determine whether hCG induces ER stress and reduces steroidogenic enzyme expression in Leydig cells *in vivo*, various dosages of hCG were administered to male mice by i.p. injection. As expected, 3β-HSD and p50ATF6 were down- and upregulated respectively in the testis upon hCG or Tm treatment (Fig. 6A). In addition, expression of p50ATF6 protein in testes of mice treated with hCG or Tm decreased upon addition of TUDCA (Fig. 6A). On the other hand, TUDCA treatment recovered the reduced expression of 3β-HSD protein upon hCG (0.5 IU/g BW per day) or Tm treatment (1.0 µg/g BW) after 3 days (Fig. 6A and B). Interestingly, the mRNA levels of *Star*, *Cyp11a1*, *3β-Hsd*, and *Cyp17* as well as the protein level of 3β-HSD dramatically increased in the testis upon low-level administration of hCG (0.05 IU/g BW per day) for 3 or 6 days compared with mice treated with saline control (Fig. 6A

and B). However, testes displayed markedly lower mRNA expression of steroidogenic enzymes, especially *3β-Hsd*, *Cyp17*, and *17β-Hsd*, upon high-level hCG (0.5 IU/g BW per day) treatment for 1 or 3 days compared with low-level hCG (0.05 IU/g BW per day) treatment (Fig. 6A and B). Further, addition of TUDCA combined with high-level hCG treatment recovered the mRNA expression of *3β-Hsd*, *Cyp17*, and *17β-Hsd* compared with high-level hCG treatment alone (Fig. 6A and B). However, there was no rescue effect of steroidogenic enzyme expression observed upon Tm treatment due to the high toxicity of Tm in Leydig cells.

Next, we investigated testosterone production in sera of mice administered hCG (0.05 and 0.5 IU/g BW) and Tm (0.2 and 1.0 µg/g BW) once per day for 3 days. The testosterone level decreased in the testis upon high-level administration of hCG (0.5 IU/g BW per day) compared with control (Fig. 6C). This result was similar with the protein level of 3β-HSD and mRNA levels of steroidogenic enzymes (Fig. 6A, B and C). Further, addition of TUDCA restored the serum level of testosterone following hCG treatment (Fig. 6C). These results indicate that high-level administration of hCG induced ER stress, which down-regulated the expression of specific steroidogenic enzymes and decreased testosterone biosynthesis eventually in Leydig cells of the testis.

p50ATF6 reduces the expression of steroidogenic enzymes in mouse testis

To confirm whether hCG-induced ER stress via the ATF6 pathway reduces the expression of steroidogenic enzymes *in vivo*, we overexpressed the *p50Atf6* gene in ICR mouse testis using LV-mediated gene transfer. Our previous research has demonstrated LV-mediated gene transfer into testis tissue, as the foreign gene was strongly expressed in Leydig cells (Kim *et al.* 2010). The testes of an ICR mouse were injected with LV-Turbor GFP or LV-p50ATF6 by microinjection, after which the injected testes with LVs were analyzed for steroidogenic enzyme expression. As shown in Fig. 7A, p50ATF6 protein was highly expressed in the testes injected with pLV-p50ATF6 compared with normal testes or those injected with LV-Turbor GFP. However, the level of *Cyp11a1*, *Cyp17*, *17β-Hsd*, and *3β-hsd* mRNAs as well as that of 3-HSD protein significantly decreased in testes injected with LV-p50ATF6 compared with normal testis or those injected with LV-Turbor GFP (Fig. 7A and B). These results demonstrate that hCG-induced ER stress via the ATF6 pathway reduced the steroidogenic enzyme, especially 3β-HSD expression, *in vivo*.
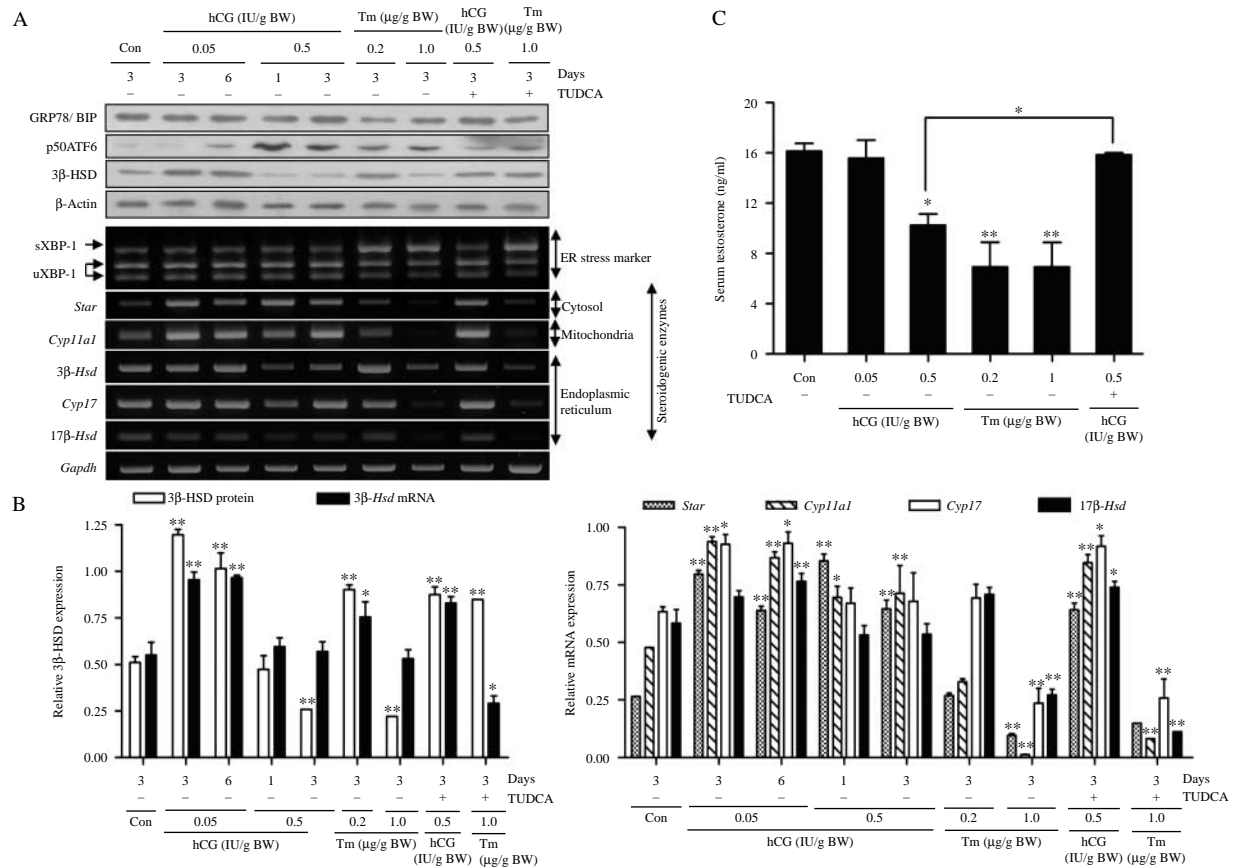
Figure 6

Administration of hCG upregulates p50ATF6 expression and down-regulates steroidogenic enzymes in Leydig cells of the testis *in vivo*. (A) Western blot analysis of GRP78/BIP, 3β-HSD, p50ATF6, and β-actin proteins along with RT-PCR analysis of sXBP1 mRNA as an ER stress marker as well as *Star*, *Cyp11a1*, *3β-hsd*, *Cyp17*, and *17β-hsd* mRNA as steroidogenic enzyme markers in testes treated with hCG, Tm, and TUDCA at the indicated concentrations and for the indicated periods. Mice were administered i.p. injection of hCG (0.05 and 0.5 IU/g BW) and tumicamycin (Tm, 0.2 and 1.0 μg/g BW) once per day. TUDCA as an ER stress inhibitor was applied by i.p. injection at the same time points (250 mg/kg at 0900 and 2000 h, total 500 mg/kg per day). Control was administrated saline by i.p. injection. (B) Graph shows that the 3β-HSD protein level was quantified and normalized to β-actin for western blot analysis. The *3β-hsd* mRNA level was quantified and normalized to GAPDH for RT-PCR analysis in testes treated with hCG, Tm, and TUDCA at the indicated concentrations and for the indicated times (left panel). Graph shows that *Star*, *Cyp11a1*, *Cyp17*, and *17β-hsd* mRNA levels were quantified and normalized to β-actin for RT-PCR analysis (right panel). Data in the bar graph represent mean ± s.e.m of three independent measurements. *$P<0.05$; **$P<0.01$, compared with control (saline). (C) Testosterone analysis in serum of ICR mice administered hCG (0.05 and 0.5 IU/g BW) and Tm (0.2 and 1.0 μg/g BW) once per day for 3 days. Serum was analyzed with a testosterone EIA kit. Data in the bar graph represent mean ± s.e.m. of three independent measurements. *$P<0.05$; **$P<0.01$.

Discussion

In males, hCG is used as a source of LH activity to stimulate testosterone production and secretion by Leydig cells of the testis. As such, hCG is used clinically to increase the body's plasma testosterone level (Depenbusch *et al*. 2002). In addition, hCG is used to stimulate testes of men who suffer from hypogonadotropic hypogonadism, cryptorchidism, or sexual dysfunction due to a lack of sufficient testosterone (Namiki 1996, Gautam *et al*. 2007). However, the side effects of excess hCG stimulation associated with overloaded ER function have never been reported. In this study, we demonstrated for the first time in detail that hCG-induced ER stress plays an important role in steroidogenic enzyme expression through the activation of UPR pathways, and excess hCG exposure induces ER stress-mediated apoptosis in mLTC-1 cells and mouse testis.

It is well known that UPR signaling plays an important role in the maturation of secretory cell types, including antibody-producing plasma cells, collagen-secreting osteo-blasts, and insulin-secreting pancreatic β-cells. As such, UPR signaling has been shown to regulate the production of
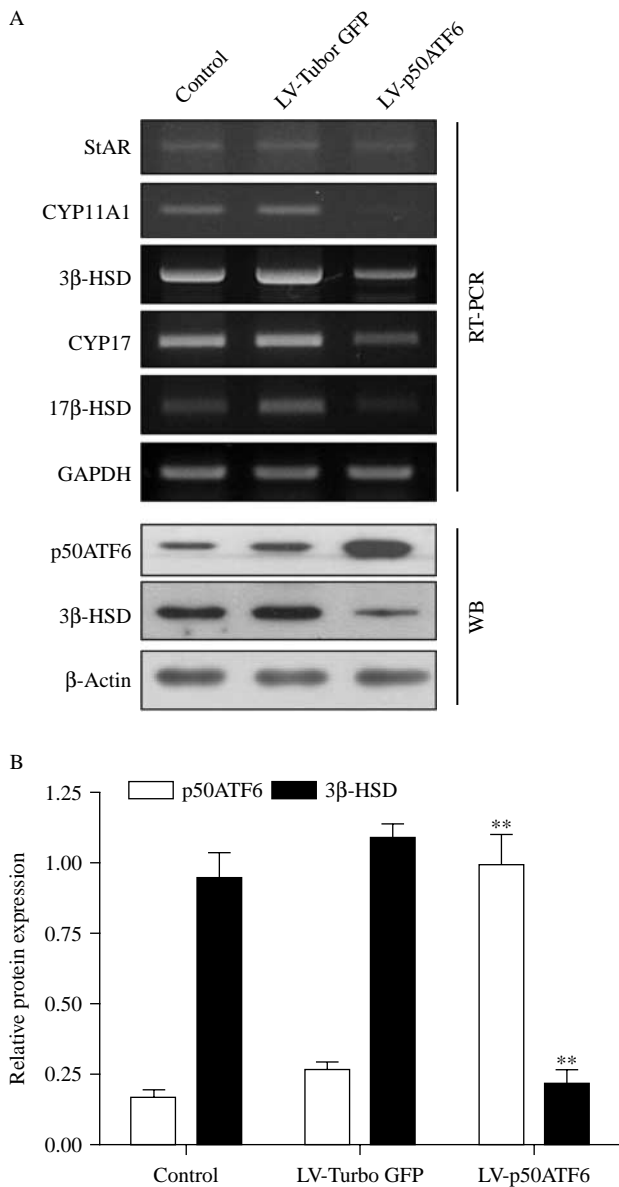
Published by Bioscientifica Ltd.

Figure 7

p50ATF6 reduces steroidogenic enzyme expression in mouse testis *in vivo*. (A) Lentiviral vector for p50ATF6, Tubor GFP, and saline (as control) injected into the testes. Four days after injection, mRNA and protein levels of the indicated genes in the testes were prepared and analyzed by RT-PCR and western blotting (WB). (B) 3β-HSD and p50ATF6 proteins were quantified and normalized to β-actin for western blot analysis. Data in the bar graph represent mean±s.ε.м. of three independent measurements. **$P<0.01$, compared with control.

specific proteins under homeostatic regulation (Wu & Kaufman 2006). As Leydig cells require continuous steroidogenic enzyme synthesis for the production of testosterone, UPR signaling also occurs upon hCG-stimulated steroidogenic enzyme expression in Leydig cells.

The expression of *Grp78/Bip* as a trigger of the UPR remarkably increased at 3 h after 5 IU/ml hCG treatment in Leydig cells (Fig. 3A upper panel). In addition, the altered expression pattern of 3β-HSD protein was in agreement with that of GRP78/BIP (Fig. 3A and C). As shown in Fig. 5A, *Grp78/Bip* expression already increased in untreated control mouse testes under physiological regulation (or basal level or hormonal regulation). These observations suggest that the ER of Leydig cells generated adaptive signaling pathways, such as the UPR, in order to maintain steroidogenic enzyme expression. Therefore, this study demonstrated for the first time that hCG induces the UPR through ATF6, IRE1a/XBP1, and elf2a/GADD34/ATF4 in Leydig cells (Fig. 3A and B).

When β-cells are exposed to conditions that induce mild ER stress, the ER can facilitate stress mitigation and restore protein homeostasis. It has been shown that IRE1α and PERK are the primary transducers for regulating insulin production under these conditions, thus promoting activation of the UPR pro-survival pathway (Fonseca *et al.* 2011). However, prolonged ER stress-induced activation of ATF6 has been shown to impair cAMP-stimulated hepatic gluconeogenesis in the liver (Seo *et al.* 2010) along with insulin synthesis in pancreatic β-cells (Seo *et al.* 2008). Therefore, we examined which of the three different UPR signaling pathways is related to the impairment of steroidogenic enzyme expression. For this, we identified which of the three UPR transcription factors (p50ATF6, ATF4, and sXBP1) mediates downregulation of 3β-HSD expression upon hCG treatment in Leydig cells. As a result, transient expression of p50ATF6 mainly downregulated the level of 3β-HSD protein in mLTC-1 cells (Fig. 4A, Supplementary Figure 3). In addition, as shown in Fig. 7, 3β-HSD protein and steroidogenic enzyme mRNA levels significantly decreased in mouse testes microinjected with LV-p50ATF6 compared with normal testes (control) or those microinjected with LV-Turbo GFP. These results suggest that hCG-induced ER stress inhibited the expression of steroidogenic enzymes through the ATF6 pathway in Leydig cells. Although the mechanism of repression of 3β-HSD and steroidogenic enzyme expression by p50ATF6 remains unclear, ATF6 may be activated by hCG-induced intracellular cAMP in Leydig cells. A previous study reported that ER stress influences hepatic gluconeogenesis, through the inhibition of cAMP-mediated activation of CREB activity induced by ATF6 (Seo *et al.* 2010). Inhibition of PKC, PKA, and phospholipase C has been shown to significantly reduce steroid production as well as phosphorylation of CREB protein in Leydig tumor cell lines (Jo *et al.* 2005). Therefore, there is a

possibility that the ATF6 pathway plays an important role in the regulation of 3β-HSD expression through inhibition of CREB activity. However, additional studies are needed to elucidate the mechanism by which the ATF6 pathway acts on CREB to regulate steroidogenic enzyme expression.

Although the UPR mediates physiological regulation or homeostasis of the ER, it can also mediate apoptotic signaling pathways under excessive ER stress (Fonseca *et al.* 2011). Specifically, ATF6, IRE1, and PERK, which are three UPR signaling factors, serve as mediators of ER stress-mediated apoptosis (Szegezdi *et al.* 2006, Lai *et al.* 2007). CHOP, p-JNK, and caspase-3 are activated by PERK/ATF6, IRE1α/TRAF2/ASK1, and caspase-12 respectively, resulting in cell apoptosis (Lai *et al.* 2007). Here, we demonstrated that hCG dramatically induced phospho-JNK, cleaved caspase-12, and CHOP protein expression at 12 h following hCG treatment (Fig. 2A). Further, cleaved caspase-3 as a mitochondrial-mediated apoptotic molecule was upregulated at 24 h after hCG treatment (Fig. 2B). *In vivo*, testes of mice treated with hCG displayed upregulation of phospho-JNK, cleaved caspase-12, CHOP, and cleaved caspase-3 expression. Interestingly, these increased levels of apoptotic molecules in the testis following hCG treatment were reduced by the addition of TUDCA (Fig. 5A). Consequently, the reduced expression of steroidogenic enzymes in the testis and subsequent decrease in the serum testosterone levels following hCG treatment were restored by TUDCA (Fig. 6).

Furthermore, ER stress has been shown to induce apoptotic morphological features, such as swelling of the ER lumen, dissociation of ribosomes from the rough ER, nuclear fragmentation, disordered mitochondria, and abnormal and/or destruction of tissue by histological analysis (Hitomi *et al.* 2004). Further, it has been reported that ER stress-mediated damage to cell or tissue morphology can be rescued by chemical chaperones such as TUDCA (Seyhun *et al.* 2011). Thus, damage to the ER and mitochondria induced by ER stress-mediated apoptosis in response to high-level administration of hCG *in vivo* resulted in fragmentation of the ER and mitochondria in Leydig cells along with abnormal histology of the testis, although this was reversed by TUDCA (Fig. 5B). Damage to the mitochondria by hCG treatment could be explained by apoptotic cross talk between the ER and mitochondria via regulation of BCL2 protein by both JNK and CHOP (Szegezdi *et al.* 2006, Lai *et al.* 2007). Therefore, prolonged hCG treatment might have induced ER stress-mediated apoptosis as well as mitochondrial apoptosis. We will attempt to identify the exact mitochondrial apoptosis pathway in a further study.

Through H&E staining analysis, we demonstrated that high-level administration of hCG (0. 5 IU/g BW) damaged both the interstitial space and the inside of seminiferous tubules (Fig. 5B). These results indicate that high-level hCG treatment induces damage to Leydig cells as well as germ cells. Based on our results, repeated and/or excessive hCG clinical treatment seems to induce ER stress and downregulate steroidogenic enzyme expression through the ATF6 pathway of UPR signaling in Leydig cells. The lasting pharmacological effects of high-dose hCG seems to induce ER stress-mediated apoptosis and reduce testosterone production in Leydig cells of the testes. Therefore, there is a possibility that high-level hCG treatment impairs steroidogenesis as well as spermatogenesis.

A 50% reduction in testis size was reported in a transgenic mouse model overexpressing both hCGα and β subunits (Matzuk *et al.* 2003), which can be explained by ER stress-mediated apoptosis. Previous studies have demonstrated that the steroidogenic capacity of aged Leydig cells is reduced by about 50% due to ROS derived from the mitochondrial electron transport chain, steroidogenesis, and/or macrophages (Allen *et al.* 2004, Chen *et al.* 2009). Testosterone production by Leydig cells occurs over the lifetime of a normal adult man, and this process may be accompanied by continuous ER stress in the testis. Based on the results of this study, prolonged ER stress induced by long-term expression of steroidogenic enzymes, which is necessary for the production of testosterone, promotes apoptosis, resulting in a gradual decline of testosterone in aged Leydig cells. In our experiment, mice treated with a high level of hCG displayed ER stress-mediated apoptosis in their testes (Fig. 5) as well as low plasma testosterone levels (Fig. 6) compared with control mice, although this was reversed by addition of TUDCA (Figs 5 and 6). Therefore, it can be concluded that TUDCA enhances the adaptive capacity of the ER and acts as a potent steroidogenic factor with potential applicability to the treatment of disrupted Leydig cells.

In conclusion, this study demonstrated, for the first time, the role of ER stress in steroidogenic enzyme expression in Leydig cells. Further, hCG-induced ER stress via the ATF6 pathway plays an important role in the expression of steroidogenic enzymes, especially 3β-HSD. High or prolonged hCG treatment induces ER stress-mediated apoptosis, which promotes a progressive decline in testosterone and steroidogenic enzyme production in Leydig cells of the testis. In addition, TUDCA as a chemical chaperone and ER stress inhibitor can rescue hCG-induced

ER stress-mediated apoptosis as well as restore production of steroidogenic enzyme and testosterone.

References

Aggarwal A, Misro MM, Maheshwari A, Sehgal N & Nandan D 2009 Adverse effects associated with persistent stimulation of Leydig cells with hCG *in vitro*. *Molecular Reproduction and Development* **76** 1076–1083. (doi:10.1002/mrd.21074)

Aggarwal A, Misro MM, Maheshwari A, Sehgal N & Nandan D 2010 *N*-acetylcysteine counteracts oxidative stress and prevents hCG-induced apoptosis in rat Leydig cells through down regulation of caspase-8 and JNK. *Molecular Reproduction and Development* **77** 900–909. (doi:10.1002/mrd.21232)

Aggarwal A, Misro MM, Maheshwari A & Sehgal N 2012 Differential modulation of apoptotic gene expression by *N*-acetyl-L-cysteine in Leydig cells stimulated persistently with hCG *in vivo*. *Molecular and Cellular Endocrinology* **348** 155–164. (doi:10.1016/j.mce.2011.08.002)

Allen JA, Diemer T, Janus P, Hales KH & Hales DB 2004 Bacterial endotoxin lipopolysaccharide and reactive oxygen species inhibit Leydig cell steroidogenesis via perturbation of mitochondria. *Endocrine* **25** 265–275. (doi:10.1385/ENDO:25:3:265)

Ascoli M, Fanelli F & Segaloff DL 2002 The lutropin/choriogonadotropin receptor, a 2002 perspective. *Endocrine Reviews* **23** 141–174. (doi:10.1210/er.23.2.141)

Chen H, Ge RS & Zirkin BR 2009 Leydig cells: from stem cells to aging. *Molecular and Cellular Endocrinology* **306** 9–16. (doi:10.1016/j.mce.2009.01.023)

Depenbusch M, von Eckardstein S, Simoni M & Nieschlag E 2002 Maintenance of spermatogenesis in hypogonadotropic hypogonadal men with human chorionic gonadotropin alone. *European Journal of Endocrinology* **147** 617–624. (doi:10.1530/eje.0.1470617)

Do MH, Santos SJ & Lawson MA 2009 GNRH induces the unfolded protein response in the LbetaT2 pituitary gonadotrope cell line. *Molecular Endocrinology* **23** 100–112. (doi:10.1210/me.2008-0071)

Fonseca SG, Gromada J & Urano F 2011 Endoplasmic reticulum stress and pancreatic β-cell death. *Trends in Endocrinology and Metabolism* **22** 266–274.

Gautam DK, Misro MM, Chaki SP, Chandra M & Sehgal N 2007 hCG treatment raises H_2O_2 levels and induces germ cell apoptosis in rat testis. *Apoptosis* **12** 1173–1182. (doi:10.1007/s10495-007-0060-1)

Haider SG 2004 Cell biology of Leydig cells in the testis. *International Review of Cytology* **233** 181–241. (doi:10.1016/S0074-7696(04)33005-6)

Haze K, Yoshida H, Yanagi H, Yura T & Mori K 1999 Mammalian transcription factor ATF6 is synthesized as a transmembrane protein and activated by proteolysis in response to endoplasmic reticulum stress. *Molecular Biology of the Cell* **10** 3787–3799.

Hitomi J, Katayama T, Taniguchi M, Honda A, Imaizumi K & Tohyama M 2004 Apoptosis induced by endoplasmic reticulum stress depends on activation of caspase-3 via caspase-12. *Neuroscience Letters* **357** 127–130. (doi:10.1016/j.neulet.2003.12.080)

Jiang HY & Wek RC 2005 Phosphorylation of the α-subunit of the eukaryotic initiation factor-2 (eIF2α) reduces protein synthesis and enhances apoptosis in response to proteasome inhibition. *Journal of Biological Chemistry* **280** 14189–14202. (doi:10.1074/jbc.M413660200)

Jo Y, King SR, Khan SA & Stocco DM 2005 Involvement of protein kinase C and cyclic adenosine 3′,5′-monophosphate-dependent kinase in steroidogenic acute regulatory protein expression and steroid biosynthesis in Leydig cells. *Biology of Reproduction* **73** 244–255. (doi:10.1095/biolreprod.104.037721)

Keay SD, Vatish M, Karteris E, Hillhouse EW & Randeva HS 2004 The role of hCG in reproductive medicine. *BJOG : an International Journal of Obstetrics and Gynaecology* **111** 1218–1228. (doi:10.1111/j.1471-0528.2004.00412.x)

Kim TS, Choi HS, Ryu BY, Gang GT, Kim SU, Koo DB, Kim JM, Han JH, Park CK, Her S *et al.* 2010 Real-time *in vivo* bioluminescence imaging of lentiviral vector-mediated gene transfer in mouse testis. *Theriogenology* **73** 129–138. (doi:10.1016/j.theriogenology.2009.07.028)

Kim MK, Kim HS, Lee IK & Park KG 2012 Endoplasmic reticulum stress and insulin biosynthesis: a review. *Experimental Diabetes Research* **2012** 509437. (doi:10.1155/2012/509437)

Kojima E, Takeuchi A, Haneda M, Yagi A, Hasegawa T, Yamaki K, Takeda K, Akira S, Shimokata K & Isobe K 2003 The function of GADD34 is a recovery from a shutoff of protein synthesis induced by ER stress: elucidation by GADD34-deficient mice. *FASEB Journal* **17** 1573–1575. (doi:10REF19=10.1096/fj.02-0462com)

Lai E, Teodoro T & Volchuk A 2007 Endoplasmic reticulum stress: signaling the unfolded protein response. *Physiology* **22** 193–201. (doi:10.1152/physiol.00050.2006)

Malhi H & Kaufman RJ 2011 Endoplasmic reticulum stress in liver disease. *Journal of Hepatology* **54** 795–809. (doi:10.1016/j.jhep.2010.11.005)

Manna PR, Huhtaniemi IT, Wang XJ, Eubank DW & Stocco DM 2002 Mechanisms of epidermal growth factor signaling: regulation of steroid biosynthesis and the steroidogenic acute regulatory protein in mouse Leydig tumor cells. *Biology of Reproduction* **67** 1393–1404. (doi:10.1095/biolreprod.102.007179)

Matzuk MM, DeMayo FJ, Hadsell LA & Kumar TR 2003 Overexpression of human chorionic gonadotropin causes multiple reproductive defects in transgenic mice. *Biology of Reproduction* **69** 338–346. (doi:10.1095/biolreprod.102.013953)

Morishima N, Nakanishi K, Takenouchi H, Shibata T & Yasuhiko Y 2002 An endoplasmic reticulum stress-specific caspase cascade in apoptosis. Cytochrome *c*-independent activation of caspase-9 by caspase-12. *Journal of Biological Chemistry* **277** 34287–34294. (doi:10.1074/jbc.M204973200)

Mosmann T 1983 Rapid colorimetric assay for cellular growth and survival: application to proliferation and cytotoxicity assays. *Journal of Immunological Methods* **65** 55–63. (doi:10.1016/0022-1759(83)90303-4)

Nakagawa T & Yuan J 2000 Cross-talk between two cysteine protease families. Activation of caspase-12 by calpain in apoptosis. *Journal of Cell Biology* **150** 887–894. (doi:10.1083/jcb.150.4.887)

Published by Bioscientifica Ltd.

Nakagawa T, Zhu H, Morishima N, Li E, Xu J, Yankner BA & Yuan J 2000 Caspase-12 mediates endoplasmic-reticulum-specific apoptosis and cytotoxicity by amyloid-β. *Nature* **403** 98–103. (doi:10.1038/47513)

Namiki M 1996 Recent concepts in the management of male infertility. *International Journal of Urology* **3** 249–255. (doi:10.1111/j.1442-2042.1996.tb00529.x)

Neaves WB 1978 The pattern of gonadotropin-induced change in plasma testosterone, testicular esterified cholesterol and Leydig cell lipid droplets in immature mice. *Biology of Reproduction* **19** 864–871. (doi:10.1095/biolreprod19.4.864)

Newhouse K, Hsuan SL, Chang SH, Cai B, Wang Y & Xia Z 2004 Rotenone-induced apoptosis is mediated by p38 and JNK MAP kinases in human dopaminergic SH-SY5Y cells. *Toxicological Sciences* **79** 137–146. (doi:10.1093/toxsci/kfh089)

Okabe K, Shibata Y, Mashimo T, Yuasa H, Yamanaka H, Asano M & Yoshida M 2000 Administration of human chorionic gonadotropin with a controlled-release function to immature rats for application in male infertility therapy. *Drug Development and Industrial Pharmacy* **26** 559–562. (doi:10.1081/DDC-100101268)

Ozcan U, Yilmaz E, Ozcan L, Furuhashi M, Vaillancourt E, Smith RO, Gorgun CZ & Hotamisligil GS 2006 Chemical chaperones reduce ER stress and restore glucose homeostasis in a mouse model of type 2 diabetes. *Science* **313** 1137–1140.

Payne AH & Hales DB 2004 Overview of steroidogenic enzymes in the pathway from cholesterol to active steroid hormones. *Endocrine Reviews* **25** 947–970. (doi:10.1210/er.2003-0030REF35=10.1146/annurev.biochem.73.011303.074134)

Rebois RV 1982 Establishment of gonadotropin-responsive murine leydig tumor cell line. *Journal of Cell Biology* **94** 70–76. (doi:10.1083/jcb.94.1.70)

Schroder M & Kaufman RJ 2005 The mammalian unfolded protein response. *Annual Review of Biochemistry* **74** 739–789. (doi:10.1146/annurev.biochem.73.011303.074134)

Seo HY, Kim YD, Lee KM, Min AK, Kim MK, Kim HS, Won KC, Park JY, Lee KU, Choi HS *et al*. 2008 Endoplasmic reticulum stress-induced activation of activating transcription factor 6 decreases insulin gene expression via up-regulation of orphan nuclear receptor small

heterodimer partner. *Endocrinology* **149** 3832–3841. (doi:10.1210/en.2008-0015)

Seo HY, Kim MK, Min AK, Kim HS, Ryu SY, Kim NK, Lee KM, Kim HJ, Choi HS, Lee KU *et al*. 2010 Endoplasmic reticulum stress-induced activation of activating transcription factor 6 decreases cAMP-stimulated hepatic gluconeogenesis via inhibition of CREB. *Endocrinology* **151** 561–568. (doi:10.1210/en.2009-0641)

Seyhun E, Malo A, Schafer C, Moskaluk CA, Hoffmann RT, Goke B & Kubisch CH 2011 Tauroursodeoxycholic acid reduces endoplasmic reticulum stress, acinar cell damage, and systemic inflammation in acute pancreatitis. *American Journal of Physiology. Gastrointestinal and Liver Physiology* **301** G773–G782. (doi:10.1152/ajpgi.00483.2010)

Shi Y, Vattem KM, Sood R, An J, Liang J, Stramm L & Wek RC 1998 Identification and characterization of pancreatic eukaryotic initiation factor 2 α-subunit kinase, PEK, involved in translational control. *Molecular and Cellular Biology* **18** 7499–7509.

Szegezdi E, Logue SE, Gorman AM & Samali A 2006 Mediators of endoplasmic reticulum stress-induced apoptosis. *EMBO Reports* **7** 880–885. (doi:10.1038/sj.embor.7400779)

Urano F, Wang X, Bertolotti A, Zhang Y, Chung P, Harding HP & Ron D 2000 Coupling of stress in the ER to activation of JNK protein kinases by transmembrane protein kinase IRE1. *Science* **287** 664–666. (doi:10.1126/science.287.5453.664)

Wu J & Kaufman RJ 2006 From acute ER stress to physiological roles of the unfolded protein response. *Cell Death and Differentiation* **13** 374–384. (doi:10.1038/sj.cdd.4401840)

Xie Q, Khaoustov VI, Chung CC, Sohn J, Krishnan B, Lewis DE & Yoffe B 2002 Effect of tauroursodeoxycholic acid on endoplasmic reticulum stress-induced caspase-12 activation. *Hepatology* **36** 592–601. (doi:10.1053/jhep.2002.35441)

Ye J, Rawson RB, Komuro R, Chen X, Dave UP, Prywes R, Brown MS & Goldstein JL 2000 ER stress induces cleavage of membrane-bound ATF6 by the same proteases that process SREBPs. *Molecular Cell* **6** 1355–1364. (doi:10.1016/S1097-2765(00)00133-7)

Yoshida H, Matsui T, Yamamoto A, Okada T & Mori K 2001 XBP1 mRNA is induced by ATF6 and spliced by IRE1 in response to ER stress to produce a highly active transcription factor. *Cell* **107** 881–891. (doi:10.1016/S0092-8674(01)00611-0)